doi:10.1093/brain/awp209 Brain 2009: 132; 2970–2979 | 2970

BRAIN
A JOURNAL OF NEUROLOGY

Longitudinal progression of sporadic Parkinson's disease: a multi-tracer positron emission tomography study

R. Nandhagopal,[1] L. Kuramoto,[1] M. Schulzer,[1] E. Mak,[1] J. Cragg,[1] Chong S. Lee,[1] J. McKenzie,[1] S. McCormick,[1] A. Samii,[2] A. Troiano,[1] T. J. Ruth,[3] V. Sossi,[4] R. de la Fuente-Fernandez,[1] Donald B. Calne[1] and A. J. Stoessl[1]

1 Pacific Parkinson's Research Centre, University of British Columbia & Vancouver Coastal Health, Vancouver, BC V6T2B5 Canada
2 Department of Neurology, University of Washington, Seattle, WA 98195 USA
3 TRIUMF, Wesbrook Mall, Vancouver, BC V6T 2A3 Canada
4 Department of Physics & Astronomy, University of British Columbia, Vancouver Hospital and Health Sciences Centre, Purdy Pavilion, Vancouver, BC V6T2B5 Canada

Correspondence to: A. Jon Stoessl, CM, MD, FRCPC,
Pacific Parkinson's Research Centre,
University of British Columbia,
Vancouver Hospital and Health Sciences Centre,
Purdy Pavilion,
2221 Wesbrook Mall,
Vancouver, BC,
V6T2B5 Canada
E-mail: jstoessl@interchange.ubc.ca

Parkinson's disease is a heterogeneous disorder with multiple factors contributing to disease initiation and progression. Using serial, multi-tracer positron emission tomography imaging, we studied a cohort of 78 subjects with sporadic Parkinson's disease to understand the disease course better. Subjects were scanned with radiotracers of presynaptic dopaminergic integrity at baseline and again after 4 and 8 years of follow-up. Non-linear multivariate regression analyses, using random effects, of the form $BP_{ND}(t)$ or $K_{occ}(t) = a*e^{(-bt-dA)} + c$, where BP_{ND} = tracer binding potential (nondispaceable), K_{OCC} = tracer uptake constant *a*, *b*, *c* and *d* are regression parameters, *t* is the symptom duration and *A* is the age at onset, were utilized to model the longitudinal progression of radiotracer binding/uptake. We found that the initial tracer binding/uptake was significantly different in anterior versus posterior striatal subregions, indicating that the degree of denervation at disease onset was different between regions. However, the relative rate of decline in tracer binding/uptake was similar between the striatal subregions. While an antero-posterior gradient of severity was maintained for dopamine synthesis, storage and reuptake, the asymmetry between the more and less affected striatum became less prominent over the disease course. Our study suggests that the mechanisms underlying Parkinson's disease initiation and progression are probably different. Whereas factors responsible for disease initiation affect striatal subregions differently, those factors contributing to disease progression affect all striatal subregions to a similar degree and may therefore reflect non-specific mechanisms such as oxidative stress, inflammation or excitotoxicity.

Keywords: Parkinson's disease; PET; progression; asymmetry; dopaminergic dysfunction

Abbreviations: DA = dopamine; DAT = membrane dopamine transporter; DTBZ = dihydrotetrabenazine; FD = fluoro-L-dopa; MP = methylphenidate; PET = positron emission tomography; ROIs = regions of interest

Received January 24, 2009. Revised May 20, 2009. Accepted June 26, 2009. Advance Access publication August 18, 2009

Introduction

Sporadic Parkinson's disease is a progressive neurodegenerative disease characterized by dysfunction of the nigrostriatal dopamine projection. The dopaminergic dysfunction shows regional vulnerability with an anterior-posterior gradient of severity between striatal subregions (Garnett *et al*., 1987; Brooks *et al*., 1990; Lee *et al*., 2000). In consonance with the striatal dopaminergic deficit, most patients with Parkinson's disease require treatment with dopaminergic medications at some point during the course of their illness. However, symptomatic benefits from medication might obscure the underlying neuropathological process when progression is studied using only clinical measures. To circumvent this problem, radio-tracer based *in vivo* imaging has been utilized for quantitative assessment of dopaminergic function (Brooks *et al*., 2003; Au *et al*., 2005). Although not fully established as a biomarker (Ravina *et al*., 2005), positron emission tomography (PET) offers an excellent tool for assessing the spatial and temporal patterns of dopaminergic dysfunction. Clinical, pathological and recent PET studies of Parkinson's disease progression indicate an exponential decline in tracer binding as a function of disease progression (Fearnley and Lees, 1991; Lee *et al*., 1994, 2004; Hilker *et al*., 2005). This non-linear reduction is in keeping with a higher rate of dopaminergic cell loss in the early stages of disease (Muller *et al*., 2000). However, study of disease progression using PET in a clinically heterogeneous disorder such as Parkinson's disease (Calne, 2000; Lewis *et al*., 2005) is generally hampered by design issues, such as the use of cross-sectional data or availability of only two data points: short duration of follow-up; and utilization of tracers for molecules or processes whose expression may be affected by compensatory changes (Lee *et al*., 2000). Given the variability in the clinical progression of Parkinson's disease, the use of additional serial data points would be expected to improve the precision of mathematical modelling of decline in dopaminergic function.

Using cross-sectional PET observations, we previously demonstrated that while a different level of denervation is attained, the rate of progression is similar across different striatal regions in Parkinson's disease (Lee *et al*., 2004). This finding raises the possibility that the mechanisms underlying disease progression may be different from those that account for disease initiation. An initiation factor such as a toxin or virus might result in the regionally differential loss of dopamine neurons, whose selective vulnerability may be determined by factors intrinsic to those neurons (e.g. expression of calbindin, the membrane dopamine transporter, etc.). In contrast, the further progression of Parkinson's disease may arise from factors (e.g. oxidative stress, excitotoxicity and inflammation) for which there is unlikely to be regionally selective vulnerability within the substantia nigra. However, this inference needs to be confirmed by longitudinal study of Parkinson's disease progression, as we describe here.

Using serial multi-tracer PET with [^{11}C](±)dihydrotetrabenazine [DTBZ—a vesicular monoamine transporter type 2 (VMAT2) marker], 6-[^{18}F]-fluoro-L-dopa (FD—a marker for uptake and decarboxylation of levodopa and subsequent vesicular trapping) and [^{11}C]d-*threo*-methylphenidate [MP, a marker for the membrane dopamine transporter (DAT)], we have studied the pattern of dopaminergic nerve terminal loss in Parkinson's disease over time, in order to understand better whether Parkinson's disease is likely to arise from a process that gradually engages all susceptible neurons, or whether there is an initial event that occurs some years earlier and then unleashes a secondary process responsible for ongoing progression. This multi-tracer PET method allowed us to explore changes in the spatial and temporal pattern of different facets of central dopamine processing in Parkinson's disease. The use of longitudinal data provides a more precise estimate of the natural course of dopaminergic denervation.

Materials and methods

Subjects

Patients who met the criteria for clinically definite Parkinson's disease (Calne *et al*., 1992) were recruited from the Movement Disorders clinic at the University of British Columbia (UBC) from January 1997 to June 2006. Patients were selected to represent a wide range of symptom duration. Patients with alternate diagnoses such as multiple system atrophy or stroke, or with borderline symptoms without convincing progression at follow-up were excluded. Of the original cohort ($n = 78$ for DTBZ, $n = 76$ for FD and $n = 76$ for MP scans, respectively), follow-up scans were performed 4 years ($n = 57$ for DTBZ, $n = 43$ for FD and $n = 47$ for MP scans) and 8 years ($n = 21$ for DTBZ, $n = 20$ for FD, and $n = 20$ for MP scans) following baseline. Table 1 shows the clinical characteristics of the patients. Quantitative measurements of motor function based on Purdue pegboard testing and the motor part of the Unified Parkinson's Disease Rating Scale (UPDRS), conducted at least 12 h off all anti-Parkinsonian medications, and multi-tracer PET were performed at each visit. All patients gave written informed consent and the study was approved by the UBC Ethics Committee.

Positron emission tomography

The scanning procedure, data processing and reconstruction have been described in detail elsewhere (Lee *et al*., 2000). In brief, anti-Parkinsonian medications were withheld for at least 12 h (immediate release levodopa) or 18–24 h (controlled release levodopa or dopamine agonists) prior to the scan. After overnight fasting and a standard low-protein breakfast on the day of scanning, the subjects were scanned in 3D mode with an ECAT 953B tomograph (CTI/Siemens, Knoxville, TN; reconstructed resolution ~9 mm in plane and 6 mm axially). A transmission scan with rotating ^{68}Ge rods was obtained ~10 min prior to injection of each radioligand for attenuation correction. Subjects were positioned supine with the scanner gantry parallel to the inferior orbitomeatal line and the head centred in the field of view by the aid of laser cross-beams. A moulded thermoplastic mask was fitted for each subject, to reduce head movement and for repositioning in subsequent scans. Presynaptic dopaminergic integrity was assessed utilizing DTBZ, MP and FD. Using a Harvard infusion pump, DTBZ (185 MBq in 10 ml of saline) was injected intravenously over 60 s. A series of sequential emission scans was obtained (4×1 min, 3×2 min, 8×5 min, 1×10-min) starting at tracer injection, for a total acquisition time of 60 min. Following an interval of 2.5 h (i.e. >7 half-lives for ^{11}C) to allow for radioactive decay, subjects were re-positioned and MP (185 MBq in 10 ml of saline) was injected. Scans were acquired over 60 min as above. Following an additional interval of at least 2.5 h subjects received FD (185–260 MBq in

Table 1 Clinical characteristics of subjects with sporadic Parkinson's disease[a]

Characteristics	Initial visit	At 4 years	At 8 years
No. of male and female	58, 20	44, 13	16, 5
Age (years)	60.7 ± 10.8	64.3 ± 10.5	65.7 ± 7.6
Symptom duration (years[b])	7.6 ± 5.9 (0.5–26)	12.0 ± 5.9 (4.5–26)	14.8 ± 6.2 (9–30)
Hoehn-Yahr stage	1.95 ± 0.79	2.71 ± 0.79	2.67 ± 0.75
UPDRS (total motor score)	27.38 ± 11.76	33.86 ± 9.87	33.54 ± 12.23
Side predominance (clinical asymmetry/worse side)	Right (n = 37)	Right (n = 25)	Right (n = 8)
	Left (n = 41)	Left (n = 32)	Left (n = 13)
Lateralized motor UPDRS score[c]			
Worse side	10.49 ± 4.03	14.69 ± 4.01	13.04 ± 5.11
Better side	5.37 ± 4.77	8.43 ± 4.48	9.33 ± 4.90
Purdue Pegboard score			
Worse side	10.85 ± 2.52	9.18 ± 2.56	8.25 ± 3.03
Better side	12.47 ± 2.88	10.3 ± 2.51	10.58 ± 2.21
Medication status			
Levodopa equivalent dosage (mg/day[d])	484 ± 391	786 ± 319	854 ± 318
Levodopa (either alone or in combination with other drugs)	n = 57	n = 52	n = 19
Dopamine agonists (either alone or in combination)	n = 23	n = 32	n = 13
Anticholinergics	n = 4	n = 2	n = 1
Amantadine	n = 9	n = 7	n = 6
Selegiline	n = 2	n = 0	n = 0
No anti-Parkinsonian medication	n = 15	n = 1	n = 0

a Data are given as mean ± SD unless otherwise indicated.
b Data in parentheses are the range.
c Lateralized motor UPDRS score refers to the summation of tremor, bradykinesia and rigidity scores of upper and lower limbs on either side (range from 0–36 for either side).
d Doses of 100 mg of levodopa in standard Sinemet are regarded as equivalent to 130 mg of levodopa in Sinemet CR = 70 mg of Sinemet with Catechol-O-methyl transferase (COMT) inhibitors = 90 mg of Sinemet CR with COMT inhibitors = 10 mg of Bromocriptine = 1 mg of Pramipexole or Pergolide = 5 mg of Ropinirole.
UPDRS = Unified Parkinson's Disease Rating Scale.

10 ml of saline). One hour prior to FD injection subjects received 200 mg of carbidopa orally. For subjects who were unable to complete all scans within an 8 h period, the FD scan was performed within 3 months of the other two. All scans were performed on the same scanner and the injection and scanning protocol were kept as similar as possible between the first and subsequent imaging sessions for all subjects.

Data analysis and statistics

The methods of image analysis have been described in detail elsewhere (Lee *et al*., 2000). In brief, a time-integrated image was created by averaging data obtained over the last 30 min of acquisition time (i.e. from 60–90 min for FD, from 30–60 min for DTBZ and MP); the five axial planes in which the striatum was best demonstrated were identified and averaged, to form a spatially and temporally integrated image for placement of regions of interest (ROIs). Circular ROIs (8.8-mm diameter) were manually placed along the axis of the striatum, identified visually, one on the head of the caudate nucleus, and three along the rostrocaudal axis of each putamen without overlap. Larger circular ROIs (diameter 19.4 mm) were positioned three per side over the cortex of the temporo-occipital lobe as a reference region. After realigning the dynamic sequence using Automated Image Registration (Woods *et al*., 1993), all ROIs were transferred onto the same spatially summed five axial planes for each time frame, to permit the generation of time activity curves. The same region of interest template was used for all tracers. ROI placement, although essentially the same for all scans, was optimized by minor adjustments to maximize counts for each tracer, in an attempt to place the ROIs as consistently as possible. Although no anatomical landmarks were used, the ROI placement was always performed by the same operator to ensure consistency and eliminate inter-operator variability. The FD uptake rate constant (K_{occ}) was determined by multiple time graphical method for unidirectional transport with reference tissue input function (Patlak and Blasberg, 1985; Martin *et al*., 1989). DTBZ and MP distribution volume ratios (DVR) were obtained using the tissue input Logan graphical method (Logan *et al*., 1996). Binding potentials (BP_{ND_DTBZ}, BP_{ND_MP}, ND = nondisplaceable) were determined by subtracting 1 from the DVR. For all tracers the occipital cortex was used as reference region. All scans were analysed by a single operator to maximize consistency. Follow-up scans of each subject were realigned to the baseline scans and regions of interest transferred automatically.

At each visit, a correlated set of 24 measurements was obtained (right and left side, four regions on each side and three tracers). Mean putaminal K_{occ} and BP_{ND_DTBZ}, and BP_{ND_MP} on the more and less affected sides were derived by averaging the values derived from the corresponding anterior, mid and posterior putaminal ROIs. Non-linear multivariate regression analyses, using random effects and allowing for missing data (Marshall *et al*., 2006) were used to model the longitudinal measurements of tracer binding/uptake in the striatal subregions (caudate, anterior, posterior putamen and mean putamen). As Parkinson's disease is a heterogeneous disease, random effects models were used. This technique allowed for a random curve for each patient. These models were of the form $BP_{ND}(t)$ or $K_{occ}(t) = ae^{(-bt-dA)} + c$, where a, b, c and d are regression parameters to be estimated, 'A' represents the age at symptom onset and 't' disease duration. In these models, $a\,e^{(-dA)} + c$ represents the intercept

at $t=0$ (symptom onset), 'c' represents the asymptotic level of the curve, 'b' is the decay constant affecting the curvature and 'd' reflects the influence of 'A' (the age of onset) on both the level and the curvature. The slope of the trajectory at any duration is given by $-abe^{(-bt-dA)}$. Comparisons were made between the parameter values obtained for the mean putamen and caudate, and between those obtained for the anterior versus posterior putamen, for the more and less affected sides separately. The trajectories describing the decline in tracer binding/uptake were also compared between the more and less affected striatum to determine the longitudinal evolution of the asymmetrical involvement of striatum. The relative efficiency of the longitudinal versus cross-sectional models was assessed from the estimated standard errors of the parameter b, for DTBZ binding in the anterior putamen of the less affected (better) side, derived longitudinally versus cross-sectionally from the baseline data. This relative efficiency estimates the relative proportion of patients saved by the longitudinal analysis as compared to the number of patients needed in the corresponding cross-sectional analysis to attain the same precision in the estimation of curvature b. SAS version 9.1.3 and R version 2.4.1 were used in the analysis.

Results

The 78 Parkinson's disease subjects (58 male and 20 female) presented with a wide range of symptom duration at the initial visit (range 0.5–26 years) (Table 1) and had symptom onset at age ranging from 24 to 73.8 years. Tremor predominant Parkinson's disease was observed in 33 subjects, while the remaining subjects ($n=45$) had predominantly bradykinetic form. At the second visit (at year 4), 53 subjects (41 male and 12 female) with a mean age of 65.1 ± 9.5 years were available for the assessment, while for the third visit (at year 8), 19 subjects (14 male and 5 female) with mean age of 65.8 ± 8.3 years participated. The drop out of subjects, an inherent problem in longitudinal studies, was due to death or advanced disease. Figure 1 demonstrates a typical scatter plot of BP_{ND_MP} against symptom duration in the anterior putamen of the less affected striatum and the superimposed fitted regression curve. The regression curves for the binding of all the tracers in the different striatal subregions provided good fits to the data. We had tried a number of more complicated models, but without any significant gain in fit over the exponential. Also, in comparing the full exponential model to one based on the average level of the data alone, there was a highly significant ($P<0.0001$) improvement in the fit due to the exponential model. Various other comparisons (e.g. to linear fits) were also made, and the exponential model won out in each case. The parameter estimates describing the exponential decline in tracer binding over time in the caudate versus mean putamen and in the anterior versus posterior putamen are shown in Tables 2 and 3 and in Figs 2–4.

Spatial pattern of progression: caudate versus mean putamen

More affected striatum

For the trajectories describing longitudinal progression in the caudate versus mean putamen, the intercepts $[ae^{(-dA)}+c]$ demonstrated a significant difference for the binding/uptake of all the tracers (Table 2). The asymptotic values c were different between caudate and putamen for $BP_{ND\_MP}(t)$ and for $K_{occ}(t)$ but not for $BP_{ND\_DTBZ}(t)$. No significant difference was observed in the decay constant b for the longitudinal decline in uptake/binding of any of the three tracers.

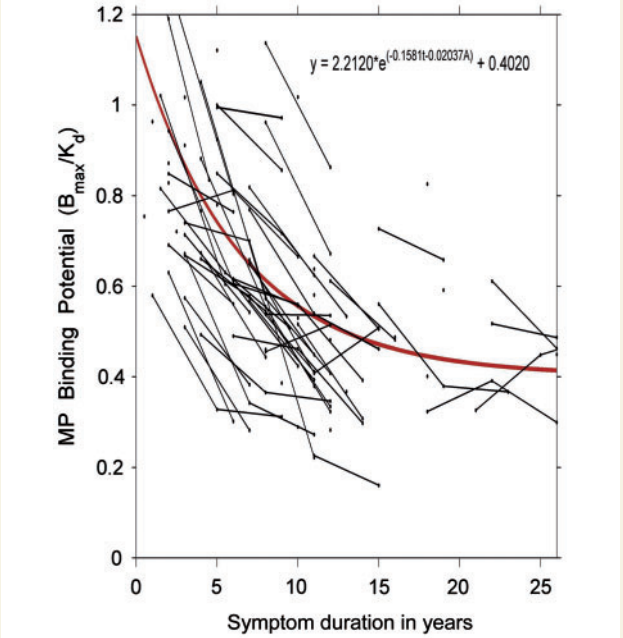

Figure 1 Individual measurements of the same subjects with sporadic Parkinson's disease are joined by straight line segments while the solid smooth line represents the fitted regression curve.

Less affected striatum

The intercepts (K_{occ} or BP_{ND} at $t=0$) were significantly different between caudate and mean putamen for all three tracers (Table 2). For FD uptake, the value of b was different between caudate and mean putamen. No significant difference was observed for the values of c.

Progression across anterior versus posterior putamen

More affected striatum

The values of K_{occ} and BP_{ND} at $t=0$ were significantly different between anterior and posterior putamen for all tracers (Table 3). Additionally, the asymptotic value c was significantly different between anterior and posterior putamen for both BP_{ND_MP} and K_{occ} (Figs 2–4).

Less affected striatum

As for the more affected striatum, values of K_{occ} and BP_{ND} at $t=0$ were significantly different between anterior and posterior putamen for all tracers and the asymptotic values were significantly different for BP_{ND_MP} and K_{occ} (Table 3, Figs 2–4).

Table 2 Comparison of longitudinal progression of radio-tracer binding between caudate and mean putamen in sporadic Parkinson's disease

Radio-tracers	Parameters	Estimates for caudate			Estimates for mean putamen			Significance levels for caudate versus mean putamen	
		More affected side[a]	Less affected side[a]	More versus less affected side[b]	More affected side[a]	Less affected side[a]	More versus less affected side[b]	More affected side[b]	Less affected side[b]
MP	Intercept	**1.060**	**1.248**	***P*<0.001**	**0.489**	**0.765**	***P*<0.001**	***P*<0.001**	***P*<0.001**
	b	**0.110**	**0.090**	NS	**0.138**	**0.148**	NS	NS	NS
	c	**0.281**	**0.249**	NS	**0.225**	**0.261**	NS	***P*=0.014**	NS
	d	0.007	0.004	NS	0.002	**0.012**	NS	***P*=0.005**	NS
FD	Intercept	**0.998**	**1.004**	NS	**0.588**	**0.747**	***P*<0.001**	***P*<0.001**	***P*<0.001**
	b	**0.127**	**0.063**	NS	**0.115**	**0.096**	NS	NS	***P*=0.012**
	c	**0.587**	**0.555**	NS	**0.214**	**0.211**	NS	***P*<0.001**	NS
	d	**−0.015**	−0.009	NS	**−0.012**	−0.007	NS	NS	NS
DTBZ	Intercept	**0.689**	**0.826**	***P*<0.001**	**0.397**	**0.594**	***P*<0.001**	***P*<0.001**	***P*<0.001**
	b	0.045	**0.061**	NS	**0.085**	**0.063**	NS	NS	NS
	c	−0.036	0.065	NS	**0.155**	0.060	NS	NS	NS
	d	−0.003	−0.003	NS	**−0.020**	**−0.007**	***P*=0.016**	***P*=0.003**	NS

a Numbers in bold indicate significant values of parameter estimates (compared to zero) across the corresponding striatal subregion.
b Numbers indicate *P*-values describing the significance of the difference between parameter estimates for caudate and putamen.

Table 3 Comparison of longitudinal progression of radio-tracer binding between anterior and posterior putamen in sporadic Parkinson's disease

Radio-tracers	Parameters	Estimates for anterior putamen			Estimates for posterior putamen			Significance levels for anterior versus posterior putamen	
		More affected side[a]	Less affected side[a]	More versus less affected side[b]	More affected side[a]	Less affected side[a]	More versus less affected side[b]	More affected side[b]	Less affected side[b]
MP	Intercept	**0.765**	**1.134**	***P*<0.001**	**0.260**	**0.440**	***P*<0.001**	***P*<0.001**	***P*<0.001**
	b	**0.140**	**0.130**	NS	0.121	**0.181**	NS	NS	NS
	c	**0.332**	**0.349**	NS	**0.128**	**0.173**	NS	***P*<0.001**	***P*<0.001**
	d	0.009	**0.016**	NS	−0.003	0.001	NS	NS	NS
FD	Intercept	**0.848**	**0.992**	***P*=0.009**	**0.330**	**0.489**	***P*<0.001**	***P*<0.001**	***P*<0.001**
	b	**0.097**	**0.072**	NS	0.107	**0.123**	NS	NS	NS
	c	**0.315**	**0.287**	NS	**0.136**	**0.154**	NS	***P*<0.001**	***P*<0.001**
	d	**−0.011**	−0.006	NS	−0.009	−0.008	NS	NS	NS
DTBZ	Intercept	**0.560**	**0.787**	***P*<0.001**	**0.247**	**0.389**	***P*<0.001**	***P*<0.001**	***P*<0.001**
	b	**0.053**	**0.058**	NS	**0.109**	0.051	NS	NS	NS
	c	0.104	0.071	NS	**0.108**	−0.019	NS	NS	NS
	d	**−0.012**	**−0.007**	NS	**−0.029**	−0.007	***P*=0.046**	NS	NS

a Numbers in bold indicate significant values of parameter estimates across the corresponding striatal subregion.
b Numbers indicate *P*-values for the comparison of the corresponding parameter estimates defining the trajectories between striatal subregions.

As the PET measurements of tracer binding/uptake in the posterior putamen might be subject to partial volume effects, we also compared the parameter estimates for anterior versus mid putamen and obtained similar findings (values at $t=0$ were significantly different for all the three tracers and the asymptotic value c was different for BP_{ND_MP} and K_{occ}, findings similar to the results obtained for the comparison of the trajectories of anterior versus posterior putamen).

Pattern of asymmetry (comparison for more versus less affected side)

Caudate

No significant difference between more and less affected caudate was observed for the values of c (Table 2 and Figs 2–4).

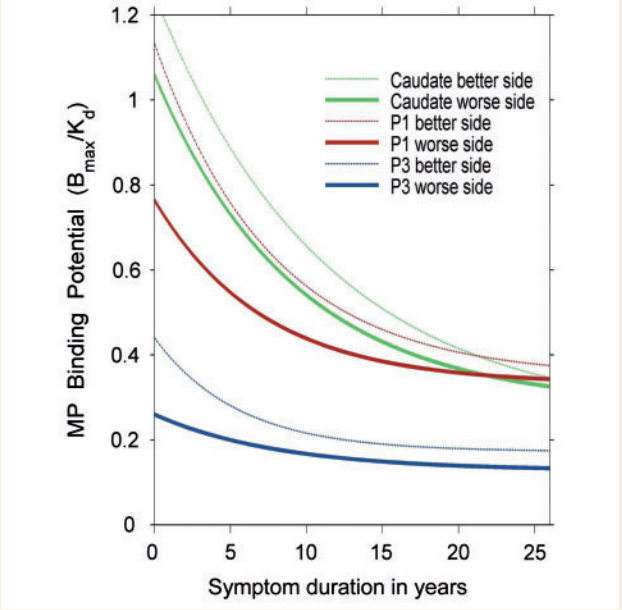

Figure 2 The three pairs of curved trajectories depict the course of decline in tracer binding in the caudate, anterior putamen (P1) and posterior putamen (P3) of more (better side) and less (worse side) affected striatum in sporadic Parkinson's disease.

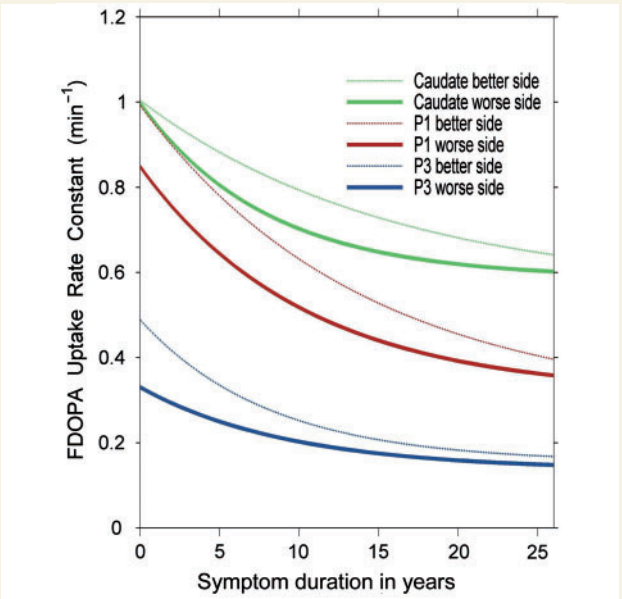

Figure 3 The three pairs of curved trajectories depict the course of decline in tracer binding in more (better side) and less (worse side) affected striatum in sporadic Parkonson's disease. FDOPA = 6-[18F]-fluoro-L-dopa P1 = anterior putamen; P3 = posterior putamen.

Anterior putamen and posterior putamen (and mean putamen)

Except for the intercept [and the value of *d* (the influence of age of onset on level and curvature) in the case of $BP_{ND\_DTBZ}(t)$], there was no significant difference in parameter estimates for more versus less affected sides for the binding of any of the three tracers in the subregions of putamen (Table 3 and Figs 2–4).

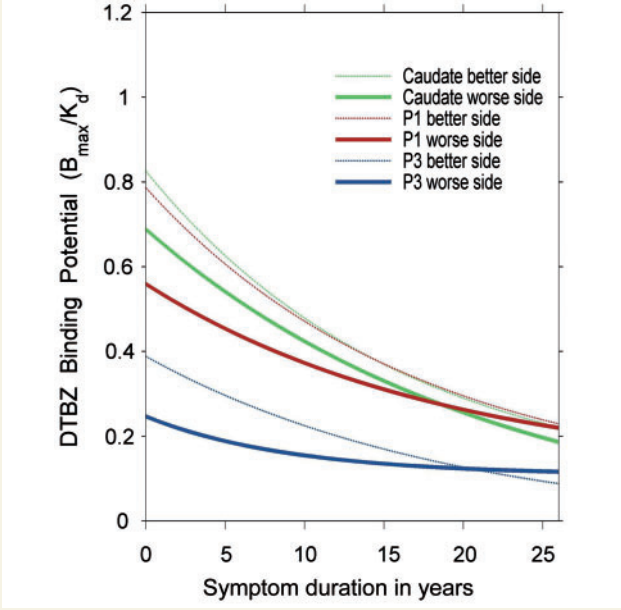

Figure 4 The three pairs of curved trajectories depict the course of decline in tracer binding in more (better side) and less (worse side) affected striatum in sporadic Parkonson's disease DTBZ = (^{11}C)(±)dihydrotetrabenazine; P1 = anterior putamen; P3 = posterior putamen.

Relative efficiency of longitudinal data in comparison with cross-sectional data

To assess the gain in efficiency from longitudinal versus cross-sectional data, we determined the standard error of the estimated curvature parameter *b* from the longitudinal analysis and the corresponding estimate based on the cross-sectional analysis of the baseline data. In the context of the BPD_{TBZ}, for example, (anterior putamen, less affected side), the relative efficiency was 5.0, indicating that the longitudinal data offered a 5-fold improvement in precision when estimating the curvature parameter *b*, with a corresponding 5-fold gain in sample size requirements. The cross-sectional analysis produced only a significant linear fit to the data.

We also carried out the analysis by including only the PET measures of those subjects who had been scanned on all three occasions. Although the power was markedly reduced, this analysis revealed essentially identical results (Fig. 5A and B).

Correlation of the change in pegboard scores, motor UPDRS and PET measurements between the visits

We examined the relationship between putamen uptake of FD and DTBZ and clinical measures, including Purdue Pegboard test and motor UPDRS scores. There was a correlation between pegboard performance and putamen uptake/binding at the first visit (for FD, worse side, Spearman's $r = 0.47$, $P < 0.001$;

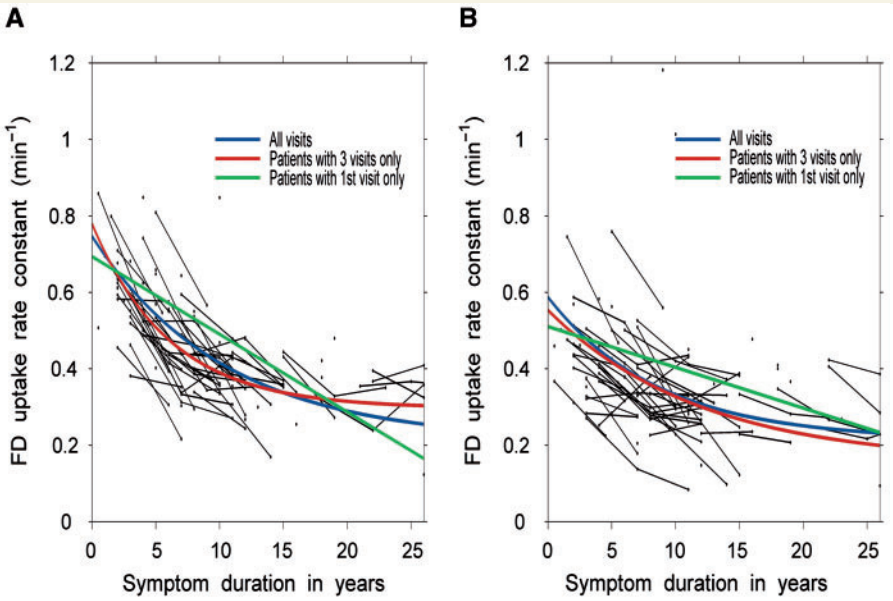

Figure 5 Trajectories of FD uptake in study participants including all subjects, subjects who had been scanned thrice longitudinally and those with PET data restricted to the first visit only. (**A**) The course in the mean putamen on the less affected striatum and (**B**) the course in the mean putamen on the more affected side.

better side, $r=0.4$, $P<0.001$; for DTBZ, worse side, $r=0.26$, $P<0.05$; better side, $r=0.34$, $P<0.005$). For motor UPDRS, similar (but inverse) correlations were found at the first visit (for FD, worse side, Spearman's $r=-0.43$, $P<0.001$; better side, $r=-0.49$, $P<0.001$; for DTBZ, worse side, $r=-0.18$, $P=$ ns; better side, $r=-0.29$, $P<0.01$). On the more affected side, these correlations were not maintained across visits. Although not all values were significant (possibly reflecting loss of power owing to subject dropout at later time points) a correlation with Pegboard performance did appear to be maintained over time on the better side, particularly in the case of FD uptake. In general, the correlations were higher for FD than for DTBZ. There was no correlation between change in pegboard performance and change in tracer uptake/binding over time.

Discussion

In this longitudinal assessment of disease progression by multi-tracer PET, we observed that dopamine denervation affects striatal subregions differently at the time of disease onset, as is evident from the significant difference in the binding/tracer uptake values at $t=0$ across regions for all tracers. In contrast, the decay constant b, which corresponds to the relative rate of decline, was similar in most regions with the possible exception of a difference in caudate versus putamen for FD uptake in the less affected striatum. The asymptotes were significantly different between anterior and posterior putamen, indicating that over the course of the illness, the antero-posterior gradient for striatal dopa influx and presynaptic reuptake of dopamine were preserved. However, the degree of side-to-side asymmetry in tracer binding between the more and less severely affected striatum becomes less prominent over the course of the illness. Previous longitudinal PET studies of Parkinson's disease progression (Morrish *et al*., 1996; Hilker *et al*., 2005; Huang *et al*., 2007) assessed striatal values that were averaged across hemispheres and have not specifically commented on the evolution of asymmetry between better and worse sides.

This longitudinal study supports the observations gleaned from an earlier cross-sectional study performed in the same cohort (Lee *et al*., 2004) in which the decay constant describing the decline in VAMT2 binding was similar across different striatal sub-regions. However, whereas both the previous and the current studies showed a significant difference in asymptotic values between anterior and posterior putamen, the present study failed to confirm the persistence of asymmetry between more and less severely affected striatum with advanced disease that was suggested in the cross-sectional study. Although similar trends were seen for DTBZ binding in the putamen, the anterior posterior gradient was surprisingly not significantly different from zero. Possible reasons could be the use of racemic (±)DTBZ with a lower dynamic range of values, and greater variance in the PET measurements, with inherently greater difficulty in parameter estimation. The latter could also account for the similar lack of statistically significant gradient for tracer binding in caudate versus mean putamen and in caudate versus posterior putamen (note that the estimated asymptotic value c was negative). While there was a correlation between PET markers of dopamine innervation and motor function at the initial visit, there was no correlation between the degree of change in clinical function and degree of change in PET marker. Several factors might contribute to the relatively poor correlation, including a lag between

the appearance of dopamine denervation and the emergence of clinical symptoms. It is to be noted that while the PET results pertain to a relatively stable measure of dopaminergic integrity at a specified point in the course of the illness, the clinical data are based on a one-time assessment performed on the day of the PET study. Variables such as patient expectation, anxiety, travel and other factors might affect the clinical score. Furthermore, the 12 h medication washout time may be insufficient to avoid some degree of persistent clinical effect. Compensatory mechanisms (or their failure) that are not captured by PET measures of dopaminergic function could also account for the lack of such correlation. Finally, clinical measures could be affected by non-dopaminergic factors.

Rate of progression in striatal subregions

The exponential pattern of tracer binding indicates that progression tends to be faster in early disease. The decline in tracer binding occurred at a similar rate across striatal subregions. This implies that the anterior-posterior gradient of dopamine dysfunction is present at disease initiation, but the striatal subregions are affected to a similar extent during disease progression.

Limitations of the study

There are several potential limitations to the current study. We did not address the progression of non-dopaminergic denervation, which may play an increasingly important role in advanced disease (Hely *et al*., 2005). Although we re-used fitted thermoplastic face masks and laser alignment to facilitate accurate repositioning of subjects between visits, minor variations in repositioning could not be avoided. This technical issue has been an inherent problem in studies employing serial PET scans (Morrish *et al*., 1996). Other potential limitations include the effects of pharmacotherapy (which of course changes over the course of a longitudinal study) on tracer binding. The potential effects of drug treatment confound all studies performed on patients with Parkinson's disease, except those restricted to the earliest stages. As outlined in Table 1, the majority of patients were on levodopa at all visits, with a progressive increase in the proportion of subjects taking dopamine agonist medication. Medications were withdrawn for 12 h prior to scanning, but it is nevertheless conceivable that medication use could alter the relationship between tracers. The relationship between tracers over time will be the subject of another paper. We have been unable to demonstrate a clear effect of dopamine agonist therapy on FD uptake (unpublished). The effects of dopaminergic therapy on DAT binding are controversial (Ahlskog *et al*., 1999; Guttman *et al*., 2001; Ravina *et al*., 2005). It is important to emphasize that the key points of the current study are (i) the exponential decline in binding/uptake of all three tracers; (ii) the maintenance of an antero-posterior gradient over the course of the illness; (iii) the ultimate loss of side-to-side asymmetry in advanced disease. As medication would presumably affect all regions of the striatum and both sides of the brain equally, points (ii) and (iii) should be insensitive to medication effects.

Patient dropouts may present a problem. The mean disease duration observed at 8 years of follow-up was somewhat shorter than might have been expected on the basis of the initial visits. However, we have applied a robust method of analysis, which is reasonably bias-resistant. Moreover, the likeliest effect of patient dropouts would have been to produce a more conservative estimate of the parameters suggesting that the remaining patients did not represent a special subset. Furthermore, the values for the parameters were similar throughout the time course. Reanalysis of the data using single and serial data points including PET measures of those subjects who had been scanned on all three occasions (Fig. 5) showed similar findings, also suggesting that the clinical course of patients who were studied at all three time-points was similar to that of other patients in the cohort. Indeed, careful cross-sectional analysis restricted to data from patients who provided only a single visit showed very similar overall rates of decay. Furthermore, in looking at the data, there is no 'funnelling' of variance over time. If there was a bias due to subject dropout, one might expect to see a reduction in variance at later time points. This also implies that there was no probable ceiling or floor effect of any importance at the time. Taken together, these observations imply that selection bias related to subject dropout is unlikely to influence the results to a significant extent.

The preferential drop out of older subjects could potentially influence the results. However, with respect to the effects of ageing, (i) age is adjusted for as a covariate in the statistical model; and (ii) in our hands, neither FD uptake nor DTBZ binding is affected by normal ageing using the methodology employed here (using plasma input, we do find an effect of age on FD uptake, but not when using a reference tissue input function).

Implications for pathogenesis of Parkinson's disease: differences between disease initiation and disease progression

The present study shows that the antero-posterior gradient of disease severity in the putamen is maintained throughout the course of Parkinson's disease, at least as estimated by DAT binding and FD uptake. However, the asymmetry between the more and less affected striatum is less pronounced with longer disease duration. The similarity of rates of disease progression in different striatal subregions supports the notion that while factors responsible for disease initiation may affect striatal subregions differently, disease progression could be due to non-specific mechanisms such as oxidative stress/free radical elaboration, excitotoxicity, mitochondrial damage, inflammation, etc. (McGeer *et al*., 1988; Jenner *et al*., 1992; Beal, 1995; Schapira *et al*., 1998; Muchowski, 2002; Tatton *et al*., 2003) that might be expected to affect striatal subregions to a similar degree. This notion is supported by the observations of progression of Parkinsonism many years after encephalitis lethargic (Calne and Lees, 1988) or after exposure to 1-methyl-4-phenyl-1,2,3,6 tetrahydropyridine (MPTP) (Langston *et al*., 1999; McGeer *et al*., 2003) associated with active inflammation. Age-related alterations in striatal dopamine

processing, neuronal attrition, mitochondrial perturbation and oxidative stress may also play a role in disease progression (Calne and Langston, 1983; Beal, 1995; Bender *et al*., 2006; Kraytsberg *et al*., 2006; Levy, 2007; Braskie *et al*., 2008). Further support for the non-specificity of mechanisms underlying progression is derived from the observation of alpha-synuclein pathology in grafted neurons many years after intrastriatal transplantation for advanced Parkinson's disease (Kordower *et al*., 2008; Li *et al*., 2008). The grafts came from donors (foetal brain) free of pre-existing Parkinson's disease. Development of α-synuclein pathology in grafted neurons suggests that they are exposed to an unfriendly milieu that contributes to neurodegeneration, much like the progression of Parkinson's disease. In fact, the finding would imply that the occurrence of Lewy bodies is not specific to early Parkinson's disease but rather that it can occur either early or related to non-specific degeneration affecting dopaminergic neurons once the environment (i.e. abnormal striatum) permits. The differential spatial pattern of involvement at symptom onset, as shown by significantly different binding/uptake values at $t=0$ across regions, and the exponential trajectories with similar decay constants b is consistent with the event hypothesis of the pathogenesis of Parkinson's disease (Schulzer *et al*., 1994). The event hypothesis envisages that a transient initial insult results in death of a limited number of neurons and damage to others, impairing their survival and normal life span. This is in contrast to the process hypothesis that assumes continuous and active destruction of healthy neurons over a prolonged period (Schulzer *et al*., 1994). It is also possible that multiple mechanisms of cell death (multiple hits) may work in concert, resulting in heterogeneity in disease onset and progression (Dawson and Dawson, 2003).

Implications for designing neuroprotective strategies/clinical trials

To the extent that PET measures reflect the clinical behaviour of disease, our findings suggest differences in the mechanisms underlying disease initiation versus progression. Hence, strategies aimed at preventing disease expression and those directed at arresting disease progression once Parkinson's disease becomes clinically manifested will need to take such differences into account.

Conclusion

Our study of disease progression in Parkinson's disease, with a large sample size at baseline and prolonged period of follow up with multi-tracer PET, confirms exponential decline in dopaminergic function and heterogeneity in the mechanism(s) responsible for disease initiation and progression. Similar longitudinal studies of asymptomatic mutation carriers of genetic forms of Parkinson's disease might provide more precise estimation of the preclinical period and might permit selection of individuals during the window of maximum potential benefit from neuroprotective interventions.

Funding

Canadian Institutes of Health Research; Michael Smith Foundation for Health Research; Canada Research Chairs program; Pacific Parkinson's Research Institute; National Parkinson Foundation.

References

Ahlskog JE, Uitti RJ, O'Connor MK, Maraganore DM, Matsumoto JY, Stark KF, et al. The effect of dopamine agonist therapy on dopamine transporter imaging in Parkinson's disease. Mov Disord 1999; 14: 940–6.

Au WL, Adams JR, Troiano AR, Stoessl AJ. Parkinson's disease: in vivo assessment of disease progression using positron emission tomography. Brain Res Mol Brain Res 2005; 134: 24–33.

Beal MF. Aging, energy, and oxidative stress in neurodegenerative diseases. Ann Neurol 1995; 38: 357–66.

Bender A, Krishnan KJ, Morris CM, Taylor GA, Reeve AK, Perry RH, et al. High levels of mitochondrial DNA deletions in substantia nigra neurons in aging and Parkinson disease. Nat Genet 2006; 38: 515–17.

Braskie MN, Wilcox CE, Landau SM, O'Neil JP, Baker SL, Madison CM, et al. Relationship of Striatal Dopamine Synthesis Capacity to Age and Cognition. J Neurosci 2008; 28: 14320–8.

Brooks DJ, Frey KA, Marek KL, Oakes D, Paty D, Prentice R, et al. Assessment of neuroimaging techniques as biomarkers of the progression of Parkinson's disease. Exp Neurol 2003; 184 (Suppl 1): S68–79.

Brooks DJ, Ibanez V, Sawle GV, Quinn N, Lees AJ, Mathias CJ, et al. Differing patterns of striatal 18F-dopa uptake in Parkinson's disease, multiple system atrophy, and progressive supranuclear palsy. Ann Neurol 1990; 28: 547–55.

Calne DB. Parkinson's disease is not one disease. Parkinsonism Relat Disord 2000; 7: 3–7.

Calne DB, Langston JW. Aetiology of Parkinson's disease. Lancet 1983; 2: 1457–9.

Calne DB, Lees AJ. Late progression of post-encephalitic Parkinson's syndrome. Can J Neurol Sci 1988; 15: 135–8.

Calne DB, Snow BJ, Lee C. Criteria for diagnosing Parkinson's disease. Ann Neurol 1992; 32 (Suppl): S125–7.

Dawson TM, Dawson VL. Molecular pathways of neurodegeneration in Parkinson's disease. Science 2003; 302: 819–22.

Fearnley JM, Lees AJ. Ageing and Parkinson's disease: substantia nigra regional selectivity. Brain 1991; 114 (Pt 5): 2283–301.

Garnett ES, Lang AE, Chirakal R, Firnau G, Nahmias C. A rostrocaudal gradient for aromatic acid decarboxylase in the human striatum. Can J Neurol Sci 1987; 14: 444–7.

Guttman M, Stewart D, Hussey D, Wilson A, Houle S, Kish S. Influence of L-dopa and pramipexole on striatal dopamine transporter in early PD. Neurology 2001; 56: 1559–64.

Hely MA, Morris JG, Reid WG, Trafficante R. Sydney Multicenter Study of Parkinson's disease: non-L-dopa-responsive problems dominate at 15 years. Mov Disord 2005; 20: 190–9.

Hilker R, Schweitzer K, Coburger S, Ghaemi M, Weisenbach S, Jacobs AH, et al. Nonlinear progression of Parkinson disease as determined by serial positron emission tomographic imaging of striatal fluorodopa F 18 activity. Arch Neurol 2005; 62: 378–82.

Huang C, Tang C, Feigin A, Lesser M, Ma Y, Pourfar M, et al. Changes in network activity with the progression of Parkinson's disease. Brain 2007; 130: 1834–46.

Jenner P, Dexter DT, Sian J, Schapira AH, Marsden CD. Oxidative stress as a cause of nigral cell death in Parkinson's disease and incidental Lewy body disease. The Royal Kings and Queens Parkinson's Disease Research Group. Ann Neurol 1992; 32 (Suppl): S82–7.

Kordower JH, Chu Y, Hauser RA, Freeman TB, Olanow CW. Lewy body-like pathology in long-term embryonic nigral transplants in Parkinson's disease. Nat Med 2008; 14: 504–6.

Kraytsberg Y, Kudryavtseva E, McKee AC, Geula C, Kowall NW, Khrapko K. Mitochondrial DNA deletions are abundant and cause functional impairment in aged human substantia nigra neurons. Nat Genet 2006; 38: 518–20.

Langston JW, Forno LS, Tetrud J, Reeves AG, Kaplan JA, Karluk D. Evidence of active nerve cell degeneration in the substantia nigra of humans years after 1-methyl-4-phenyl-1,2,3,6-tetrahydropyridine exposure. Ann Neurol 1999; 46: 598–605.

Lee CS, Samii A, Sossi V, Ruth TJ, Schulzer M, Holden JE, et al. In vivo positron emission tomographic evidence for compensatory changes in presynaptic dopaminergic nerve terminals in Parkinson's disease. Ann Neurol 2000; 47: 493–503.

Lee CS, Schulzer M, de la Fuente-Fernandez R, Mak E, Kuramoto L, Sossi V, et al. Lack of regional selectivity during the progression of Parkinson disease: implications for pathogenesis. Arch Neurol 2004; 61: 1920–5.

Lee CS, Schulzer M, Mak EK, Snow BJ, Tsui JK, Calne S, et al. Clinical observations on the rate of progression of idiopathic parkinsonism. Brain 1994; 117 (Pt 3): 501–7.

Levy G. The relationship of Parkinson disease with aging. Arch Neurol 2007; 64: 1242–6.

Lewis SJ, Foltynie T, Blackwell AD, Robbins TW, Owen AM, Barker RA. Heterogeneity of Parkinson's disease in the early clinical stages using a data driven approach. J Neurol Neurosurg Psychiatry 2005; 76: 343–8.

Li JY, Englund E, Holton JL, Soulet D, Hagell P, Lees AJ, et al. Lewy bodies in grafted neurons in subjects with Parkinson's disease suggest host-to-graft disease propagation. Nat Med 2008; 14: 501–3.

Logan J, Fowler JS, Volkow ND, Wang GJ, Ding YS, Alexoff DL. Distribution volume ratios without blood sampling from graphical analysis of PET data. J Cereb Blood Flow Metab 1996; 16: 834–40.

Marshall G, Cruz-Mesia R, Baron AE, Rutledge JH, Zerbe GO. Non-linear random effects model for multivariate responses with missing data. Stat Med 2006; 25: 2817–30.

Martin WR, Palmer MR, Patlak CS, Calne DB. Nigrostriatal function in humans studied with positron emission tomography. Ann Neurol 1989; 26: 535–42.

McGeer PL, Itagaki S, Akiyama H, McGeer EG. Rate of cell death in parkinsonism indicates active neuropathological process. Ann Neurol 1988; 24: 574–6.

McGeer PL, Schwab C, Parent A, Doudet D. Presence of reactive microglia in monkey substantia nigra years after 1-methyl-4-phenyl-1,2,3,6-tetrahydropyridine administration. Ann Neurol 2003; 54: 599–604.

Morrish PK, Sawle GV, Brooks DJ. An [18F]dopa-PET and clinical study of the rate of progression in Parkinson's disease. Brain 1996; 119 (Pt 2): 585–91.

Muchowski PJ. Protein misfolding, amyloid formation, and neurodegeneration: a critical role for molecular chaperones? Neuron 2002; 35: 9–12.

Muller J, Wenning GK, Jellinger K, McKee A, Poewe W, Litvan I. Progression of Hoehn and Yahr stages in Parkinsonian disorders: a clinicopathologic study. Neurology 2000; 55: 888–91.

Patlak CS, Blasberg RG. Graphical evaluation of blood-to-brain transfer constants from multiple-time uptake data. Generalizations. J Cereb Blood Flow Metab 1985; 5: 584–90.

Ravina B, Eidelberg D, Ahlskog JE, Albin RL, Brooks DJ, Carbon M, et al. The role of radiotracer imaging in Parkinson disease. Neurology 2005; 64: 208–15.

Schapira AH, Gu M, Taanman JW, Tabrizi SJ, Seaton T, Cleeter M, et al. Mitochondria in the etiology and pathogenesis of Parkinson's disease. Ann Neurol 1998; 44: S89–98.

Schulzer M, Lee CS, Mak EK, Vingerhoets FJ, Calne DB. A mathematical model of pathogenesis in idiopathic parkinsonism. Brain 1994; 117 (Pt 3): 509–16.

Tatton WG, Chalmers-Redman R, Brown D, Tatton N. Apoptosis in Parkinson's disease: signals for neuronal degradation. Ann Neurol 2003; 53 (Suppl 3): S61–70.

Woods RP, Mazziotta JC, Cherry SR. MRI-PET registration with automated algorithm. J Comput Assist Tomogr 1993; 17: 536–46.